# Intensity Noise and Pulse Oscillations of an InAs/GaAs Quantum Dot Laser on Germanium

Yue-Guang Zhou, *Student Member, IEEE*, Jianan Duan, *Student Member, IEEE*, Heming Huang, Xu-Yi Zhao, Chun-Fang Cao, Qian Gong, Frédéric Grillot, *Senior Member, IEEE*, and Cheng Wang, *Member, IEEE*

***Abstract*—This paper investigates the intensity noise and pulse oscillation characteristics of an InAs/GaAs quantum dot laser epitaxially grown on germanium. We show that the relative intensity noise of the free-running laser generally decreases with increasing pump current, and the minimum value reaches down to about −126 dB/Hz. The intensity noise is hardly affected by the optical feedback, unless there is a resonance or pulse oscillation in the noise spectrum. The laser pumped at a high current is more sensitive to the optical feedback. Interestingly, it is found that the free-running Ge-based quantum dot laser generates self-sustained pulse oscillations with one period or two periods upon the pump current, without incorporating saturable absorbers. This behavior is valuable for both self-generation of photonic microwaves and for understanding nonlinear dynamics of semiconductor lasers.**

***Index Terms*—Quantum dot laser, silicon photonics, intensity noise, optical feedback, Q switching, nonlinear dynamics.**

## I. Introduction

PHOTONIC integrated circuits (PICs) on silicon (Si) are developing rapidly since 2000s, owing to the large transmission bandwidth requirement in data centers, and the fast calculation speed requirement in neural networks [1]–[3]. Various optical components including optical modulators, waveguides, photodiodes, and optical switches have been successfully demonstrated on the silicon platform [4]–[6]. Nevertheless, it is still very challenging to integrate reliable semiconductor lasers on Si, because Si is inefficient for achieving stimulated emission due to its indirect bandgap structure [7], [8]. One of the most successful solutions to circumvent this problem is to integrate mature III-V semiconductor lasers on Si, thanks to the superior optical properties of III-V materials [7]. The common three integration techniques include flip-chip bonding, wafer bonding, and direct epitaxial growth [9]–[12]. In comparison with the former two methods, the latter one has a much higher potential to achieve low-cost, high-yield, and large-scale production [8]. However, the large lattice mismatch between III-V materials and Si (4% for GaAs and 8% for InP) leads to high-density threading dislocation defects, which increases the lasing threshold and reduces the aging lifetime [9], [13]. Despite that, thanks to the low sensitivity of nanostructures to epitaxial defects, both InAs/GaAs and InAs/InP quantum dot (QD) lasers have been successfully grown on Si since 2010s [8], [14]–[16]. On the other hand, taking advantage of the mature Ge-Si wafer technology, InAs/GaAs QD lasers can also be conveniently grown on germanium (Ge), owing to the small lattice mismatch between GaAs and Ge (only 0.08%) [9], [17]. In addition, Ge-based photodiodes, optical modulators and waveguides exhibit superior performances and high potential of compatibility with CMOS circuits, making the development of Ge-based QD lasers attractive as well [18]–[20].

In recent years, tremendous efforts have been devoted to improve the quality of InAs/GaAs QD lasers epitaxially grown on Si [8], [13], [21], [22]. Consequently, Ge- and Si-based QD lasers have demonstrated comparable static performances with QD lasers on native GaAs substrate, including low threshold current density [21], high temperature stability [14], and long aging lifetime [23]. In terms of dynamical performances, the relative intensity noise (RIN) and its sensitivity to optical feedback have drawn a lot of attentions, in particular because the RIN directly affects the bit error rate in the data transmission [24], [25]. On the other hand, residual optical feedback in the optical link can significantly raise the RIN level once the feedback strength exceeds the critical feedback level, which drives the laser into coherence collapse and severe chaotic oscillations [26], [27]. Consequently, an optical isolator is usually accompanied with semiconductor lasers to avoid any residual optical feedback in optical transmission systems. A. Liu *et al.* reported that a Si-based QD laser had a 20-dB reduced sensitivity to optical feedback than a quantum well laser [28]. Y. G. Zhou *et al.*

Manuscript received February 7, 2019; revised April 9, 2019 and May 10, 2019; accepted May 13, 2019. Date of publication May 17, 2019; date of current version May 31, 2019. This work was supported in part by the National Natural Science Foundation of China under Grant 61804095, in part by the Shanghai Pujiang Program under Grant 17PJ1406500, and in part by the Institute Mines-Télécom. *(Corresponding author: Cheng Wang.)*

Y.-G. Zhou is with the School of Information Science and Technology, ShanghaiTech University, Shanghai 201210, China, and also with the Laboratoire de Traitement et Communication de l'Information, Télécom ParisTech, 75013 Paris, France (e-mail: zhouyg@shanghaitech.edu.cn).

J. Duan and H. Huang are with the Laboratoire de Traitement et Communication de l'Information, Télécom ParisTech, 75013 Paris, France (e-mail: jianan.duan@telecom-paristech.fr; heming.huang@telecom-paristech.fr).

X.-Y. Zhao, C.-F. Cao, and Q. Gong are with the State Key Laboratory of Functional Materials for Informatics, Shanghai Institute of Microsystem and Information Technology, Chinese Academy of Sciences, Shanghai 200050, China (e-mail: xyzhao@mail.sim.ac.cn; ccf@mail.sim.ac.cn; qgong@mail.sim.ac.cn).

F. Grillot is with the Laboratoire de Traitement et Communication de l'Information, Télécom ParisTech, 75013 Paris, France, and also with the Center for High Technology Materials, The University of New Mexico, Albuquerque, NM 87106 USA (e-mail: grillot@telecom-paristech.fr).

C. Wang is with the School of Information Science and Technology, ShanghaiTech University, Shanghai 201210, China (e-mail: wangcheng1@shanghaitech.edu.cn).

Color versions of one or more of the figures in this paper are available online at http://ieeexplore.ieee.org.

Digital Object Identifier 10.1109/JSTQE.2019.2917548

found that the RIN of a Ge-based QD laser was 15-dB higher than a GaAs-based one, due to the high density defects [17]. On the other hand, both Ge- and Si-based lasers are also found less sensitive to the optical feedback, because the defects contribute to increasing the damping factor, which is helpful to enhance the critical feedback level [29], [30]. H. Huang *et al.* also showed that a large threshold difference between the excited state and the ground state was beneficial to enhance the optical feedback tolerance of a Si-based QD laser [30]. Besides, M. Liao *et al.* demonstrated a Si-based QD laser with a RIN of about -150 dB/Hz [31]. In addition to the large damping factor, a low linewidth broadening factor (LBF) is also helpful to reduce the phase amplitude coupling and hence the optical feedback sensitivity [32]. Recently, J. Duan *et al.* reported Si-based QD lasers with ultra-low LBFs in the range of 0.1-0.5, thanks to the improved high uniformity of QD sizes [33]. In addition, it was demonstrated that the p-doping could further reduce the LBF. For the direct modulation of Si-based QD lasers, D. Inoue *et al.* reported a 3-dB bandwidth of 6.5 GHz associated with a 12.5 Gbps non-return-zero large signal modulation [22]. Besides, C. Hantschmann *et al.* analyzed the modulation properties of a Si-based QD laser with a small-signal bandwidth of 1.6 GHz [34]. Very recently, S. Liu *et al.* demonstrated both single-section and two-section mode-locked QD lasers on Si, respectively [35], [36].

The aim of this work has two folds: on one hand, we investigate the intensity noise and its optical feedback characteristics of an InAs/GaAs QD laser epitaxially grown on Ge. On the other hand, we unveil the self-sustained pulse oscillations of the free-running Ge-based laser. The laser exhibits a LBF of 2.5 at the gain peak. Increasing the pump currents reduces the RIN down to $-126$ dB/Hz, while the optical feedback does not significantly raise the RIN for feedback levels up to 7.0%, with a round-trip optical feedback length of 42.8 m. Interestingly, the free-running Ge-based QD laser exhibits self-sustained pulse oscillations with one period or two periods, depending on the pump currents. Among these, the period-one oscillation is useful for photonic microwave generation and hence is analyzed in details. The paper is organized as follows: Section II describes the epi-layer structure of the Ge-based QD laser and its static properties. Section III discusses the RIN and its optical feedback sensitivity. Section IV investigates the self-sustained pulse oscillation characteristics, and Section V summarizes this work.

## II. Laser Structure and Static Properties

Fig. 1 shows the epi-layer structure of the InAs/GaAs QD laser epitaxially grown on Ge. A 600-nm thickness GaAs buffer layer was first grown on the Ge substrate with 6° off-cut towards [111] plane by the gas-source molecular beam epitaxy. The GaAs buffer layer restrains the propagation of epitaxial defects including anti-phase boundaries and threading dislocations into the active region. The defect density on the buffer layer surface is estimated to be around $10^6$ cm$^{-2}$, by counting the number of rhombic pinholes in the atomic force microscopy image. The active region consists of 5 stacked dot-in-well (DWELL) layers, and each layer is composed of 2.2 monolayer (ML) InAs

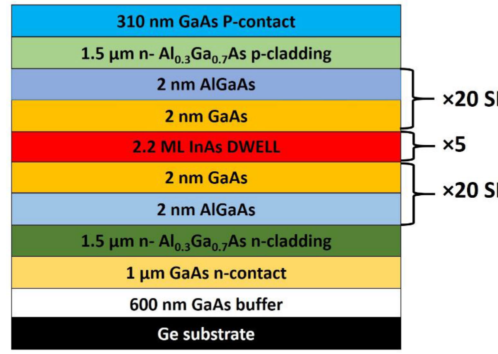


Fig. 1. Epi-layer structure of the InAs/GaAs QD laser on Ge substrate.

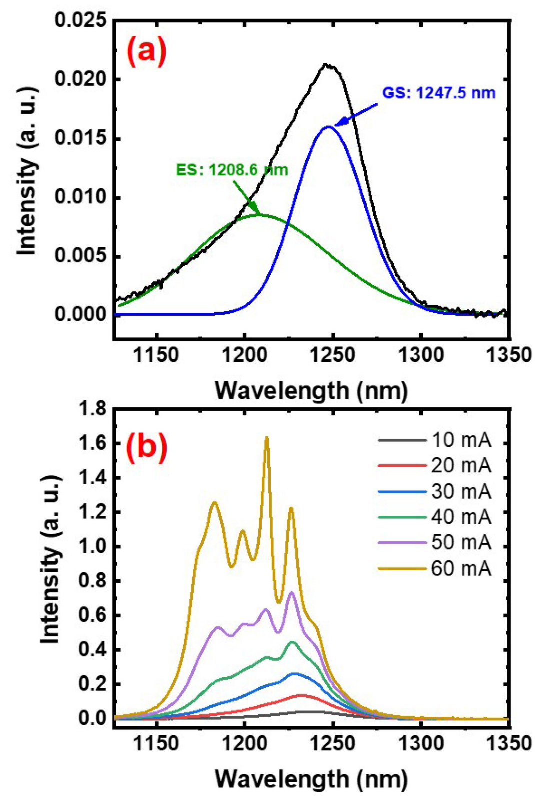


Fig. 2. (a) PL spectrum and (b) EL spectra of the Ge-based QD laser.

QDs. The dot density is about $2.0 \times 10^{10}$ cm$^{-2}$, with an average dot diameter of 61 nm and an average height of 10 nm. The laser was fabricated into ridge waveguide with a ridge width of 4.0 $\mu$m, and a cavity length of 4.4 mm. Both laser facets are left as-cleaved without any coatings [29]. Fig. 2(a) shows the photoluminescence (PL) spectrum of the Ge-based QD wafer measured at 20 °C, which shows a linewidth (full width at half maximum) of 60 nm (48 meV). The Gaussian fitting of the PL spectrum shows that the ground state (GS) peaks around 1247.5 nm, and the first excited state (ES) locates 39 nm away (32 meV). The large inhomogeneous broadening of dot size leads to the wide energy overlap between the ES and the GS. Fig. 2(b) shows the electroluminescence (EL) spectra of the laser

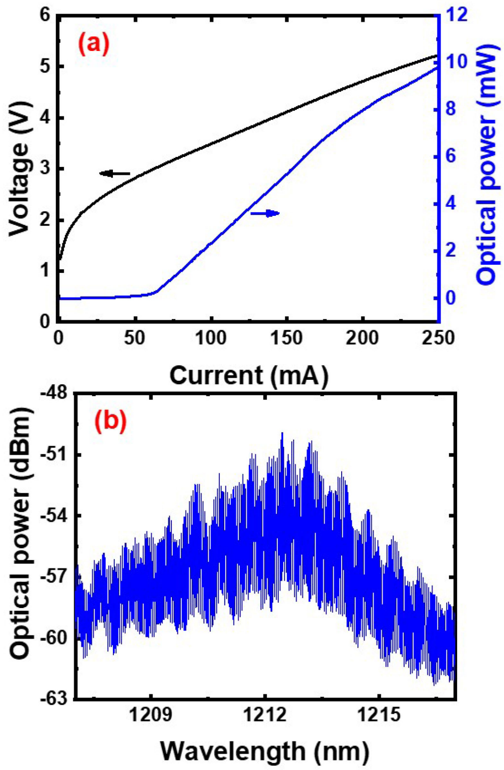


Fig. 3. (a) L-I-V curve of the Ge-based QD laser. (b) Optical spectrum at the lasing threshold.

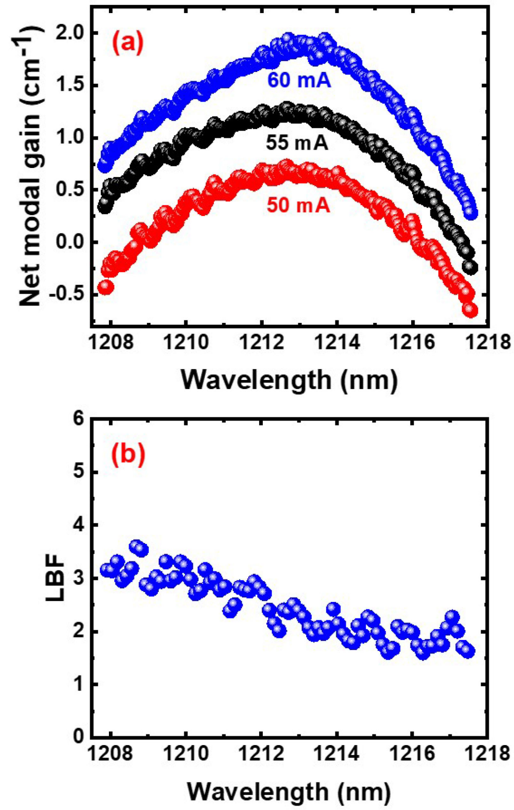


Fig. 4. (a) Net modal gain for several sub-threshold pump currents. (b) LBF of the Ge-based laser versus the lasing wavelength.

operated below the lasing threshold. Close to the threshold, the laser exhibits four distinct peaks around 1182 nm, 1200 nm, 1212 nm and 1226 nm, respectively. All the energy separations between adjacent peaks are less than 15 meV, which is much less than the GS and the ES separation. Therefore, the generation of multiple peaks is not due to the localized states. It might be because of that there are multiple groups of dots, which populate independently [37]. However, it is unclear why the homogeneous broadening does not group the dots into one ensemble [38]. Therefore, the corresponding physical mechanism still requires further exploration.

Throughout the measurements in this work, the laser operation temperature is maintained at 20 °C by a thermo-electric cooler. Fig. 3(a) shows that the Ge-based QD laser exhibits a lasing threshold of $I_{th} = 60$ mA, associated with a threshold voltage of 3.0 V. The series resistance determined by the V-I curve is 12.1 Ω. The optical spectrum at the lasing threshold in Fig. 3(b) centers around 1213 nm. The longitudinal mode spacing is 0.43 nm, resulting in a group refractive index of 3.84 and a facet power reflectivity of 0.34. Based on the Hakki-Paoli method [39], [40], Fig. 3(a) extracts the net modal gains at sub-threshold currents using the optical spectra of amplified spontaneous emission. The gain spectra are asymmetric due to the dot size dispersion, which leads to the non-zero LBF in Fig. 4(b). In the measurement of the sub-threshold LBF, the carrier-induced blue shift of the optical wavelength is extracted by carefully removing the thermal effect, which is determined by the above-threshold red-shift of the wavelength [41]. Fig. 4(b) shows that the LBF displays a relatively large sub-threshold value, which varies from about 3.0 at 1208 nm down to about 2.0 at 1218 nm, and the LBF value is 2.5 at the gain peak (1213 nm). The decreasing LBF as a function of the wavelength can be attributed to the inhomogeneous broadening of the gain medium deviating from Gaussian lineshape, as well as the carrier contribution in the higher energy states of QDs [42]. It is noted that the LBF of QD lasers operated above threshold is larger than that below threshold, and usually increases with the pump current [43], [44]. This may contribute to the rich nonlinear dynamics discussed in Section IV.

## III. Intensity Noise and Sensitivity to Optical Feedback

This section first investigates the RIN of the free-running InAs/GaAs QD lasers on Ge, and then discusses its sensitivity to optical feedback.

### A. Relative Intensity Noise

The RIN of the Ge-based QD laser is measured through converting the optical signal into electrical one using a fast photodiode with a bandwidth of 10 GHz. The electrical spectrum of the intensity noise is measured on a broadband electrical spectrum analyzer (Rohde& Schwarz FSU43), and the DC electrical power is tracked on a multimeter [17]. Fig. 5(a) shows the

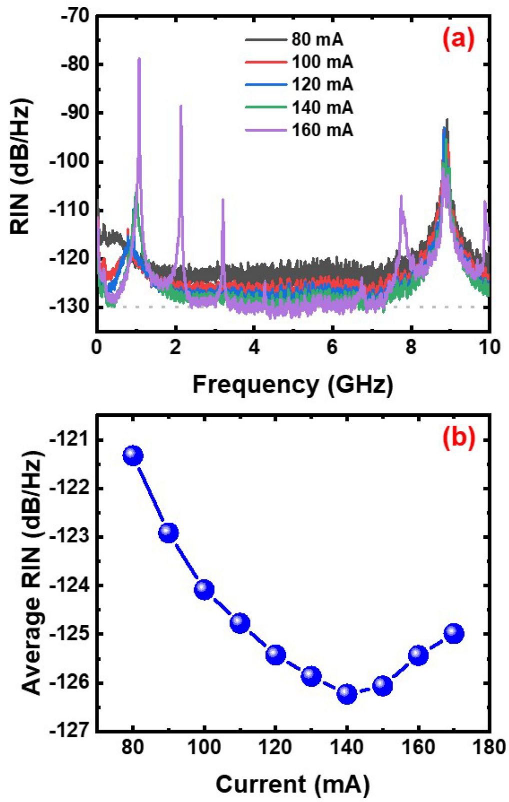


Fig. 5. (a) RIN spectra of the Ge-based QD laser at several pump currents. (b) Averaged RIN values within 10 GHz as a function of the pump current.

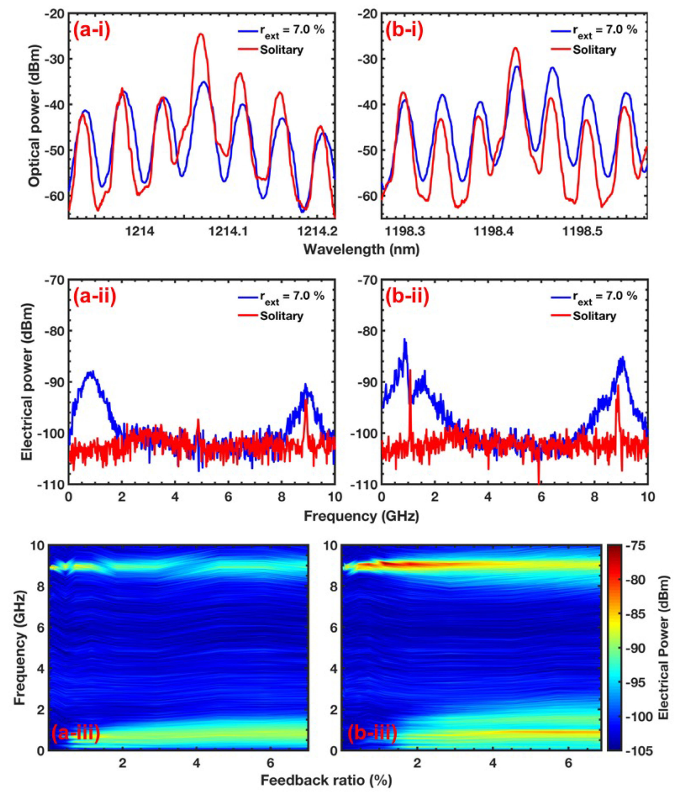


Fig. 6. Optical feedback dynamics of the Ge-based QD laser at (a) $1.5 \times I_{th}$ and at (b) $2.5 \times I_{th}$, respectively. The first row is the optical spectrum and the second one is the electrical spectrum, with ($r_{ext} = 7.0\%$) and without optical feedback. The third row is the electrical power distribution map formed by the feedback ratio and the microwave frequency.

measured RIN spectra of the Ge-based laser at several pump currents. At 80 mA, the laser exhibits a clear relaxation oscillation resonance at 0.4 GHz, where the RIN is amplified. In the frequency range of 2.0–7.0 GHz, the RIN becomes almost constant. Interestingly, a broad peak appears at 8.9 GHz, corresponding to the free spectral range of the Fabry-Perot laser. This phenomenon is recognized as the photon-photon resonance (PPR), which originates from the quasi-phase locking of multiple longitudinal modes [45]–[47]. The quasi-phase locking mechanism is usually provided by gratings including distributed feedback and Bragg reflector [48], [49]. The PPR has been widely explored to enhance the modulation bandwidth of semiconductor lasers, in combination with the relaxation oscillation resonance [50], [51]. However, it is not common to observe the PPR in a Fabry-Perot cavity. The quasi-phasing locking mechanism in this laser can be attributed to high third-order nonlinear susceptibility of QDs, which leads to strong four-wave mixing effect [52]–[54]. The high third-order susceptibility has been proved to be responsible for the self mode-locking commonly observed in single-section QD lasers [35], [55]–[57]. Unlike grating lasers, the PPR frequency of the tested Fabry-Perot laser does not increase with the pump current, because cavity length does not change. On the other hand, increasing current enhances the relaxation oscillation frequency. However, the resonance peak becomes sharper and higher instead of being overdamped. Finally, the resonance peak evolves into pulse oscillations, which will be discussed in details in Section IV. The RIN value averaged over 10 GHz in Fig. 5(b) reduces with the pump current from $-121.3$ dB/Hz at 80 mA down to the minimum level of $-126.2$ dB/Hz at 140 mA. Above 140 mA, the averaged RIN re-increases due to the appearance of multiple peaks shown in Fig. 5(a).

### *B. Sensitivity to External Optical Feedback*

In order to investigate the external optical feedback sensitivity of the Ge-based laser, we employ a commercial back-reflector (EXFO BKR) to provide optical feedback with a tunable feedback ratio $r_{ext}$ up to 7.0% [30]. The round-trip optical feedback length is fixed at 42.8 m. Fig. 6 presents the optical feedback characteristics of the Ge-based laser pumped at $1.5 \times I_{th}$ (Fig. 6(a)) and $2.5 \times I_{th}$ (Fig. 6(b)), respectively. At a feedback ratio of about 7.0%, the amplitudes of some longitudinal modes are raised while the others are suppressed, due to the interaction with external cavity modes [58], [59]. At a feedback ratio of about 7.0%, the spectral linewidth of the laser does not show any significant broadening, indicating no clear transition towards the chaotic regime (e.g., coherence collapse). The electrical spectra in Fig. 6(a-ii) and Fig. 6(b-ii) prove that the optical feedback raises the intensity noise both around the oscillation resonance (1.0 GHz) and around the PPR (8.9 GHz). On the other hand,

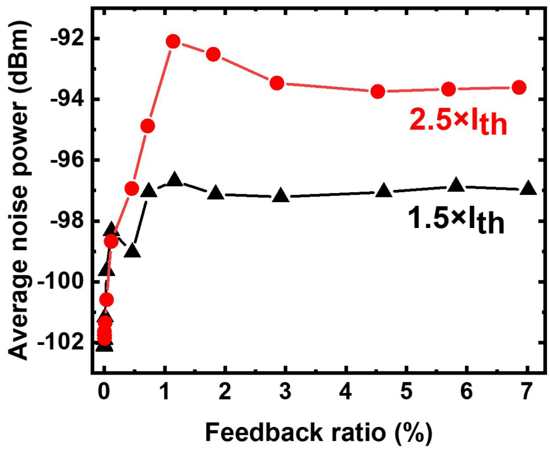


Fig. 7. Averaged intensity noise power within 10 GHz as a function of feedback ratio at 1.5 × $I_{th}$ and 2.5 × $I_{th}$, respectively.

optical feedback has little impact on the flat part of the intensity noise. The electrical power distributions in Fig. 6(a-iii) and Fig. 6(b-iii) show that both the relaxation oscillation peak and the PPR peak are broadened significantly at 2.5 × $I_{th}$ than at 1.5 × $I_{th}$, although the optical spectra are not broadened. Therefore, it is hard to exclude the presence of chaotic oscillations under this feedback condition [27], [60]–[63]. Fig. 7 shows that the average intensity noise within 10 GHz is significantly raised by the weak optical feedback up to 1.0%: from −102.1 dBm to −96.7 dBm at 1.5×$I_{th}$, and from −101.8 dBm to −92.1 dBm at 2.5 × $I_{th}$. Interestingly, the intensity noise for both currents becomes relatively insensitive to the optical feedback with feedback ratio above 1.0%. The measured noise powers at 2.0 × $I_{th}$ and at 3.0 × $I_{th}$ exhibit similar behavior as well. Obviously, the Ge-based laser is more sensitive to the optical feedback at higher pump currents, as usually observed in multimode QD lasers [29], [32], [62], [64]. This can be attributed to the larger LBF, the heavier thermal effect, as well as increased number of lasing modes [27], [44], [65]. It is worthwhile to mention that the intensity noise in Fig. 7 does not show a kink, above which the feedback significantly raises the noise level [66].

## IV. Self-Sustained Pulse Oscillations

QD lasers incorporating a saturable absorber can generate pulse oscillations, owing to the passive Q-switching mechanism [67]–[69]. Because the carrier lifetime of QDs is in the nanosecond range, the resulted pulsation frequency is usually around 1.0 GHz range. Particularly, Viktorov *et al.* observed a period doubling sequence of bifurcations to chaos in a two-state QD laser with a saturable absorber [70]. Interestingly, a QD laser without an absorber section was observed to show self-sustained pulsations [71]. The pulse generation was attributed to the large overlap between the GS and the ES of QDs, where unsaturated GS provided saturable absorption for the laser emission from the ES.

Fig. 5(a) has shown that the relaxation resonance peak of the free-running laser became less damped at a higher pump current, and evolved into self-sustained pulse oscillation at 140 mA and 160 mA. The phenomenon is analogous to the laser dynamics in the vicinity of Hopf bifurcation when the laser is subject to optical injection or optical feedback, although the corresponding mechanisms are different [27], [72]. In the range of 140–190 mA, the free-running QD laser exhibits pulse oscillations with one period in the time domain. As an example, the laser pumped at 170 mA in Fig. 8(a) shows a fundamental oscillation frequency at $f_0 = 1.09$ GHz on the electrical spectrum (left column). The corresponding time series (middle column) and the phase portrait (right column) clearly show the feature of period-one oscillation. Increasing the pump current enhances the amplitude of the microwave peak. When the laser is pumped in the range of 190–200 mA (see 196 mA in Fig. 8(b)), a sub-harmonic peak appears at half of the fundamental frequency in the electrical spectrum. Meanwhile, the time series exhibits two periods and the corresponding phase portrait shows two cycles, verifying the period-two oscillation. Further increase of the pump current to the range of 200–220 mA (see 210 mA in Fig. 8(c)) slightly enhances the fundamental frequency ($f_0$=1.11 GHz at 210 mA). In addition, the amplitude of the sub-harmonic peak in the electrical spectrum is raised as well. The electrical spectrum in Fig. 8(c) has no qualitative difference with Fig. 8(b), which can be continuously and smoothly transformed to each other. Thus, Fig. 8(c) is period-two oscillation as well. However, the corresponding time series and the phase portrait are deformed, where two loops about the center of the orbit are required to complete one period. When the laser is operated in 220–230 mA, the fundamental frequency slightly decreases, and the amplitude of the sub-harmonic peak reduces as well. Further increasing the pump current to the range of 230–250 mA (see 240 mA in Fig. 8(d)), the laser undergoes an inverse period-doubling bifurcation back to period-one oscillation as shown in the electrical spectrum. The fundamental frequency slightly increases with increasing pump current ($f_0 = 1.25$ GHz at 240 mA). On the other hand, both the time series and the phase portrait are strongly deformed.

It is found that the evolution of the self-sustained pulse oscillations of the Ge-based QD laser in Fig. 8 is closely related to the variation of the optical spectra in Fig. 9. The optical spectra in Fig. 9(a) show multiple peaks, as suggested in the EL spectra in Fig. 2(b). When the laser is operated in the continuous-wave range (60–140 mA), the two peaks with shorter wavelengths $P_{1,2}$ are far below the lasing threshold, while the three peaks with longer wavelengths $P_{3,4,5}$ are above threshold and hence emit photons. When the laser is operated in the pulse oscillation range (140–250 mA), the peaks $P_{3,4,5}$ have little power variation, and hence the generation of pulse oscillations is less likely related to these three peaks. On the other hand, the main change of the optical spectrum in this range is that the peak $P_1$ becomes lasing. Therefore, we believe the pulse oscillation dynamics is governed (at least partially) by the evolution of the peak $P_1$. The generation of $P_1$ might be due to the carrier population in a separate group of dots, like the generation of other peaks. Another possible reason is that $P_1$ emission comes from the carrier population in the ES, because the separation (43 nm) between $P_1$ and $P_5$ is similar to the ES and GS separation (39 nm) in the PL spectrum in Fig. 2(a). In addition, we believe the peak

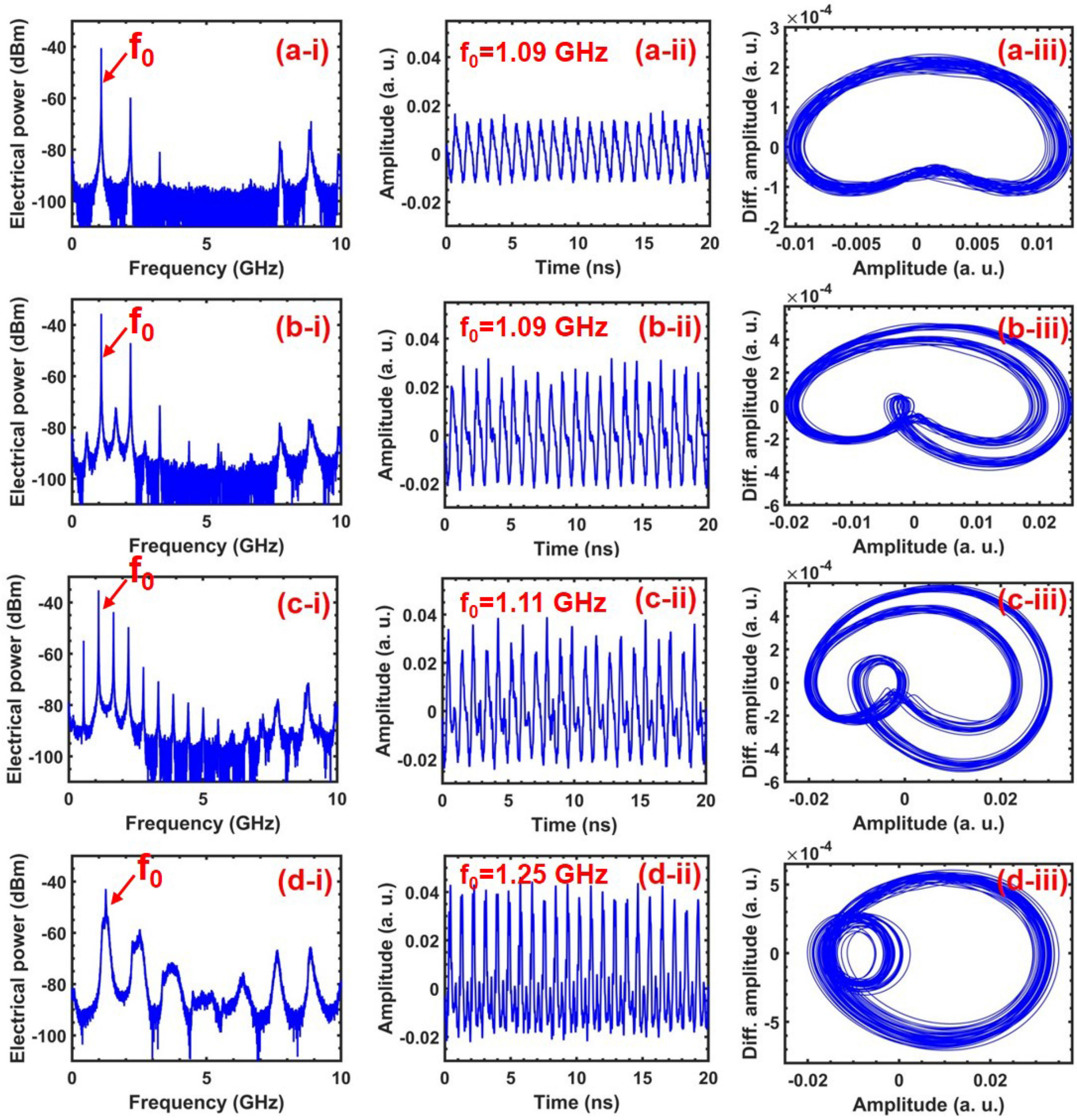


Fig. 8. Electrical spectra (left), time series (middle), and phase portraits (right) of the free-running Ge-based laser at (a) 170 mA, (b) 196 mA, (c) 210 mA, and (d) 240 mA.

$P_2$ plays a crucial role in the pulsation dynamics as well, which remains below threshold in the whole current range. Therefore, the states governing $P_2$ are only partially populated, and hence unsaturated. The separation between $P_1$ and $P_2$ is only 10 nm (9.0 meV). Thus, it is not surprising that the states governing $P_1$ have some overlap with those governing $P_2$, due to the large inhomogeneous broadening (see Fig. 2). Consequently, the unsaturated states of $P_2$ can provide saturable absorption for the overlapped states of $P_1$ once it becomes lasing. It suggests that the Q-switch mechanism is responsible for the pulsation dynamics observed in Fig. 8. The time-varying loss level induced by the unsaturated states of $P_2$ is dependent on both the pump current and the emitted photon density from $P_1$ [73]. The Q-switching mechanism is similar to the pulsation reported in [71], where the unoccupied GS acts as a saturable absorber for the QD laser emission from the ES. However, that laser does not show period-two oscillations.

When the Ge-based laser is operated in the regime of 140–190 mA, $P_1$ is only slightly above the lasing threshold and emits a weak optical power, leading to the generation of period-one oscillation. Increasing the pump current enhances the optical power of $P_1$, and hence increases the microwave power in Fig. 8(a). The optical power of $P_1$ keeps increasing in the regime of 190–230 mA, resulting in period-two oscillation. When the laser is operated above 230 mA, the optical power of $P_1$ becomes weak, driving the laser back to period-one oscillation. It is remarked that another tested laser with a cavity length of 2.2 mm exhibits similar pulsation behavior, which shows multiple peaks in the optical spectrum as well. However, not all Ge-based QD lasers produce self-sustained pulsations, depending on the structure of the optical spectrum.

The period-one pulse oscillation at 140–190 mA in Fig. 8(a) can be used for the generation of photonic microwaves [74]–[77]. Fig. 10(a) shows the frequency and the power of the

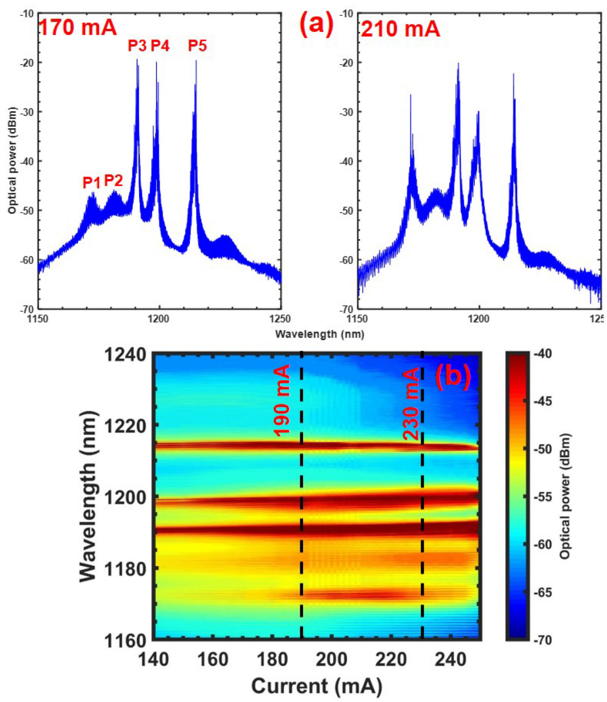


Fig. 9. (a) Optical spectra at 170 mA (left) and 210 mA (right). (b) Optical power distribution map versus pump currents. Dashed lines indicate pump currents of 190 mA and 230 mA, respectively.

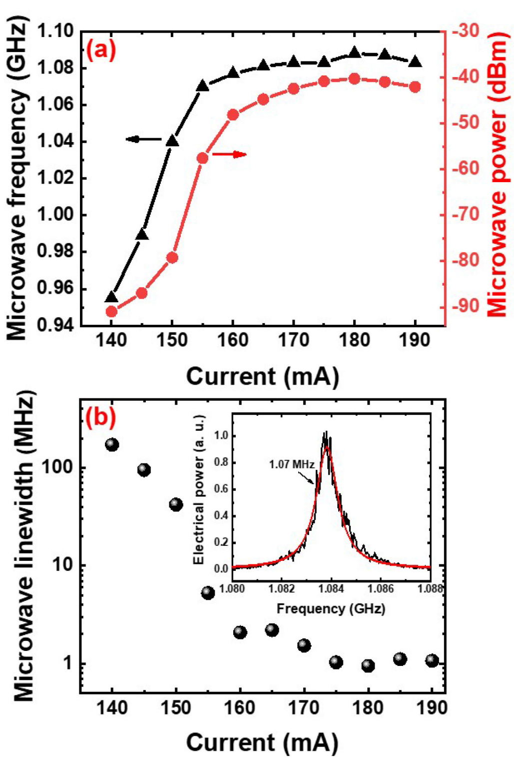


Fig. 10. Photonic microwave generated by the period-one pulse oscillation. (a) Microwave frequency and power. (b) Microwave linewidth as a function of the pump currents. The inset in (b) shows the lineshape of the microwave at 190 mA.

generated microwave as a function of the pump currents. It is shown that the microwave frequency slightly increases from 0.96 GHz at 140 mA to 1.08 GHz at 170 mA. Meanwhile, the microwave power significantly goes up from −91 dBm to −42 dBm. At above 170 mA, both the microwave frequency and the microwave power only vary slightly. On the other hand, the microwave linewidth in Fig. 10(b) decreases with the pump currents from 171.6 MHz at 140 mA down to 1.5 MHz at 170 mA. The decreasing microwave linewidth can be (partly) attributed to the reduction of laser phase noise with increasing pump current. Similar to the frequency and power, the linewidth also has little variation above 170 mA, which saturates around 1.0 MHz (see inset of Fig. 10(b)). It is remarked that the PPR peak at 8.9 GHz may distort the quality of the microwave signal generated by the period-one oscillations. This problem can be circumvented by employing a microwave filter to purify the microwave.

## V. Conclusion

In summary, we investigate the dynamical characteristics of the intensity noise and the self-sustained pulse oscillations of an InAs/GaAs QD laser epitaxially grown on Ge. The laser shows a sub-threshold LBF of 2.5 at the gain peak. The minimum RIN of the laser is around −126 dB/Hz. When the laser is subject to optical feedback, the intensity noise is hardly affected except at the resonance or pulse oscillation peak. We also demonstrate that the laser pumped at high currents is more sensitive to the optical feedback. In addition, we unveil that the free-running Ge-based QD laser exhibits self-sustained pulse oscillations, emerging from the undamped relaxation oscillations. The pulse oscillations exhibit one period or two periods, depending on the pump currents. The generation of the self-sustained pulse oscillation is qualitatively attributed to the Q-switching mechanism. Finally, we show that both the microwave power and frequency produced by the period-one oscillation increase with the pump currents, while the microwave linewidth is reduced down to about 1.0 MHz. Future work will theoretically investigate the self-sustained pulse oscillation behavior through numerical simulations, which can offer an in-depth insight on the corresponding physical mechanisms.

## Acknowledgment

The authors would like to thank Prof. Fan-Yi Lin at National Tsing Hua University for very helpful discussions.

## References

[1] P. Dong, Y.-K. Chen, G.-H. Duan, and D. T. Neilson, "Silicon photonic devices and integrated circuits," *Nanophotonics*, vol. 3, no. 4-5, pp. 215–228, 2014.

[2] K. Nishi, K. Takemasa, M. Sugawara, and Y. Arakawa, "Development of quantum dot lasers for data-com and silicon photonics applications," *IEEE J. Sel. Topics Quantum Electron.*, vol. 23, no. 6, Nov./Dec. 2017, Art. no. 1901007.

[3] X. Lin *et al.*, "All-optical machine learning using diffractive deep neural networks," *Science*, vol. 361, no. 6406, pp. 1004–1008, 2018.

[4] J. Cardenas *et al.*, "Low loss etchless silicon photonic waveguides," *Opt. Express*, vol. 17, no. 6, pp. 4752–4757, 2009.

[5] G. T. Reed, G. Mashanovich, F. Y. Gardes, and D. Thomson, "Silicon optical modulators," *Nature Photon.*, vol. 4, no. 8, pp. 518–526, 2010.
[6] J. Michel, J. Liu, and L. C. Kimerling, "High-performance Ge-on-Si photodetectors," *Nature Photon.*, vol. 4, no. 8, pp. 527–534, 2010.
[7] D. Liang and J. E. Bowers, "Recent progress in lasers on silicon," *Nature Photon.*, vol. 4, no. 8, pp. 511–517, 2010.
[8] S. Chen *et al.*, "Electrically pumped continuous-wave III-V quantum dot lasers on silicon," *Nature Photon.*, vol. 10, no. 5, pp. 307–311, 2016.
[9] H. Liu *et al.*, "Long-wavelength InAs/GaAs quantum-dot laser diode monolithically grown on Ge substrate," *Nature Photon.*, vol. 5, no. 7, pp. 416–419, 2011.
[10] K. Tanabe, T. Rae, K. Watanabe, and Y. Arakawa, "High-temperature 1.3 $\mu$m InAs/GaAs quantum dot lasers on Si substrates fabricated by wafer bonding," *Appl. Phys. Express*, vol. 6, no. 6, 2013, Art. no. 082703.
[11] Y. Urino *et al.*, "First demonstration of athermal silicon optical interposers with quantum dot lasers operating up to 125 °C," *J. Lightw. Technol.*, vol. 33, no. 6, pp. 1223–1229, Mar. 2015.
[12] G. Kurczveil, D. Liang, M. Fiorentino, and R. G. Beausoleil, "Robust hybrid quantum dot laser for integrated silicon photonics," *Opt. Express*, vol. 24, no. 14, pp. 16167–16174, 2016.
[13] Y. Wang *et al.*, "Monolithic quantum-dot distributed feedback laser array on silicon," *Optica*, vol. 5, no. 5, pp. 528–533, 2018.
[14] A. Y. Liu *et al.*, "High performance continuous wave 1.3 $\mu$m quantum dot lasers on silicon," *Appl. Phys. Lett.*, vol. 104, no. 4, 2014, Art. no. 041104.
[15] J. Kwoen *et al.*, "All MBE grown InAs/GaAs quantum dot lasers on on-axis Si (001)," *Opt. Express*, vol. 26, no. 9, pp. 11568–11576, 2018.
[16] Y. Han *et al.*, "Room-temperature InP/InGaAs nano-ridge lasers grown on Si and emitting at telecom bands," *Optica*, vol. 5, no. 8, pp. 918–923, 2018.
[17] Y.-G. Zhou *et al.*, "Relative intensity noise of InAs quantum dot lasers epitaxially grown on Ge," *Opt. Express*, vol. 25, no. 23, pp. 28817–28824, 2017.
[18] L. Vivien *et al.*, "42 GHz p.i.n germanium photodetector integrated in a silicon-on-insulator waveguide," *Opt. Express*, vol. 17, no. 8, pp. 6252–6257, 2009.
[19] S. Assefa *et al.*, "CMOS-integrated high-speed MSM germanium waveguide photodetector," *Opt. Express*, vol. 18, no. 5, pp. 4986–4999, 2010.
[20] P. Chaisakul *et al.*, "Integrated germanium optical interconnects on silicon substrates," *Nature Photon.*, vol. 8, no. 6, pp. 482–488, 2014.
[21] A. Y. Liu *et al.*, "Electrically pumped continuous-wave 1.3 $\mu$m quantum-dot lasers epitaxially grown on on-axis (001) GaP/Si," *Opt. Lett.*, vol. 42, no. 2, pp. 338–341, 2017.
[22] D. Inoue *et al.*, "Directly modulated 1.3 $\mu$m quantum dot lasers epitaxially grown on silicon," *Opt. Express*, vol. 26, no. 6, pp. 7022–7033, 2018.
[23] D. Jung *et al.*, "Impact of threading dislocation density on the lifetime of InAs quantum dot lasers on Si," *Appl. Phys. Lett.*, vol. 112, no. 15, 2018, Art. no. 153507.
[24] L. A. Coldren, S. W. Corzine, and M. L. Mashanovitch, *Diode Lasers and Photonic Integrated Circuits*. Hoboken, NJ, USA: Wiley, 2012, chs. 2–5.
[25] J. Duan, X.-G. Wang, Y.-G. Zhou, C. Wang, and F. Grillot, "Carrier-noise-enhanced relative intensity noise of quantum dot lasers," *IEEE J. Quantum Electron.*, vol. 54, no. 6, Dec. 2018, Art. no. 2001407.
[26] F. Grillot *et al.*, "2.5-Gb/s transmission characteristics of 1.3-$\mu$ m DFB lasers with external optical feedback," *IEEE Photon. Technol. Lett.*, vol. 14, no. 1, pp. 101–103, Jan. 2002.
[27] J. Ohtsubo, *Semiconductor Lasers: Stability, Instability and Chaos*. New York, NY, USA: Springer, 2012.
[28] A. Y. Liu, T. Komljenovic, M. L. Davenport, A. C. Gossard, and J. E. Bowers, "Reflection sensitivity of 1.3 $\mu$m quantum dot lasers epitaxially grown on silicon," *Opt. Express*, vol. 25, no. 9, pp. 9535–9543, 2017.
[29] Y.-G. Zhou, X.-Y. Zhao, C.-F. Cao, Q. Gong, and C. Wang, "High optical feedback tolerance of InAs/GaAs quantum dot lasers on germanium," *Opt. Express*, vol. 26, no. 21, pp. 28131–28139, 2018.
[30] H. Huang *et al.*, "Analysis of the optical feedback dynamics in InAs/GaAs quantum dot lasers directly grown on silicon," *J. Opt. Soc. Am. B*, vol. 35, no. 11, pp. 2780–2787, 2018.
[31] M. Liao *et al.*, "Low-noise 1.3 $\mu$m InAs/GaAs quantum dot laser monolithically grown on silicon," *Photon. Res.*, vol. 6, no. 11, pp. 1062–1066, 2018.
[32] S. Azouigui *et al.*, "Optical feedback tolerance of quantum-dot- and quantum-dash-based semiconductor lasers operating at 1.55 $\mu$m," *IEEE J. Sel. Topics Quantum Electron.*, vol. 15, no. 3, pp. 764–773, May/Jun. 2009.
[33] J. Duan *et al.*, "Semiconductor quantum dot lasers epitaxially grown on silicon with low linewidth enhancement factor," *Appl. Phys. Lett.*, vol. 112, no. 25, 2018, Art. no. 251111.
[34] C. Hantschmann *et al.*, "Understanding the bandwidth limitations in monolithic 1.3 $\mu$m InAs/GaAs quantum dot lasers on silicon," *J. Lightw. Technol.*, vol. 37, no. 3, pp. 949–955, Feb. 2019.
[35] S. Liu *et al.*, "490 fs pulse generation from passively mode-locked single section quantum dot laser directly grown on on-axis GaP/Si," *Electron. Lett.*, vol. 54, no. 7, pp. 432–433, 2018.
[36] S. Liu *et al.*, "Monolithic 9 GHz passively mode locked quantum dot lasers directly grown on on-axis (001) Si," *Appl. Phys. Lett.*, vol. 113, no. 4, 2018, Art. no. 041108.
[37] D. Bimberg, M. Grundmann, and N. N. Ledentsov, *Quantum Dot Heterostructures*. New York, NY, USA: Wiley, 1999.
[38] M. Sugawara, K. Mukai, Y. Nakata, H. Ishikawa, and A. Sakamoto, "Effect of homogeneous broadening of optical gain on lasing spectra in self-assembled $In_x$ $Ga_{1-x}$ As/GaAs quantum dot lasers," *Phys. Rev. B*, vol. 61, pp. 7595–7603, 2000.
[39] M. Osinski and J. Buus, "Linewidth broadening factor in semiconductor lasers—An overview," *IEEE J. Quantum Electron.*, vol. QE-23, no. 1, pp. 9–29, Jan. 1987.
[40] C. Wang, K. Schires, M. Osiński, P. J. Poole, and F. Grillot, "Thermally insensitive determination of the linewidth broadening factor in nanostructured semiconductor lasers using optical injection locking," *Sci. Rep.*, vol. 6, 2016, Art. no. 27825.
[41] F. Lelarge *et al.*, "Room temperature continuous-wave operation of buried ridge stripe lasers using InAs-InP (100) quantum dots as active core," *IEEE Photon. Technol. Lett.*, vol. 17, no. 7, pp. 1369–1371, Jul. 2005.
[42] M. Gioannini, A. Sevega, and I. Montrosset, "Simulations of differential gain and linewidth enhancement factor of quantum dot semiconductor lasers," *Opt. Quantum Electron.*, vol. 38, nos. 4–6, pp. 381–394, 2006.
[43] C. Wang, M. Osinski, J. Even, and F. Grillot, "Phase-amplitude coupling characteristics in directly modulated quantum dot lasers," *Appl. Phys. Lett.*, vol. 105, no. 22, 2014, Art. no. 221114.
[44] C. Wang, J.-P. Zhuang, F. Grillot, and S.-C. Chan, "Contribution of off-resonant states to the phase noise of quantum dot lasers," *Opt. Express*, vol. 24, no. 26, pp. 29872–29881, 2016.
[45] U. Feiste, "Optimization of modulation bandwidth in DBR lasers with detuned Bragg reflectors," *IEEE J. Quantum Electron.*, vol. 34, no. 12, pp. 2371–2379, Dec. 1998.
[46] A. Laakso and M. Dumitrescu, "Modified rate equation model including the photon-photon resonance," *Opt. Quantum Electron.*, vol. 42, no. 11-13, pp. 785–791, 2011.
[47] M. Dumitrescu, A. Laakso, S. Afzal, and P. Bardella, "Development of high-speed directly modulated DFB and DBR lasers with surface gratings," *Proc. SPIE*, vol. 7953, no. 1, pp. 643–648, 2011.
[48] P. Bardella and I. Montrosset, "A new design procedure for DBR lasers exploiting the photon-photon resonance to achieve extended modulation bandwidth," *IEEE J. Sel. Topics Quantum Electron.*, vol. 19, no. 4, Jul./Aug. 2013, Art. no. 1502408.
[49] T. Uusitalo, H. Virtanen, P. Bardella, and M. Dumitrescu, "Analysis of the photon–photon resonance influence on the direct modulation bandwidth of dual-longitudinal-mode distributed feedback lasers," *Opt. Quantum Electron.*, vol. 49, no. 1, p. 46, 2017.
[50] W. Kaiser, L. Bach, J. P. Reithmaier, and A. Forchel, "High-speed coupled-cavity injection grating lasers with tailored modulation transfer functions," *IEEE Photon. Technol. Lett.*, vol. 16, no. 9, pp. 1997–1999, Sep. 2004.
[51] B. Hong, T. Kitano, T. Mori, H. Jiang, and K. Hamamoto, "Bandwidth enhancement scheme demonstration on direct modulation active-MMI laser diode using multiple photon photon resonance," *Appl. Phys. Lett.*, vol. 111, no. 22, 2017, Art. no. 221105.
[52] H. Su *et al.*, "Nondegenerate four-wave mixing in quantum dot distributed feedback lasers," *IEEE Photon. Technol. Lett.*, vol. 17, no. 8, pp. 1686–1688, Aug. 2005.
[53] C. Wang *et al.*, "Nondegenerate four-wave mixing in a dual-mode injection-locked InAs/InP (100) nanostructure laser," *IEEE Photon. J.*, vol. 6, no. 1, Feb. 2014, Art. no. 1500408.
[54] H. Huang *et al.*, "Efficiency of four-wave mixing in injection-locked InAs/GaAs quantum-dot lasers," *AIP Adv.*, vol. 6, no. 12, 2016, Art. no. 125105.
[55] J. Renaudier *et al.*, "45 GHz self-pulsation with narrow linewidth in quantum dot Fabry-Perot semiconductor lasers at 1.5 $\mu$m," *Electron. Lett.*, vol. 41, no. 18, pp. 1007–1008, 2005.
[56] R. Rosales *et al.*, "InAs/InP quantum-dot passively mode-locked lasers for 1.55-$\mu$ m applications," *IEEE J. Sel. Topics Quantum Electron.*, vol. 17, no. 5, pp. 1292–1301, Sep./Oct. 2011.

[57] P. Bardella, L. L. Columbo, and M. Gioannini, “Self-generation of optical frequency comb in single section quantum dot Fabry-Perot lasers: A theoretical study,” *Opt. Express*, vol. 25, no. 21, pp. 26234–26252, 2017.

[58] J. M. Buldú *et al.*, “Asymmetric and delayed activation of side modes in multimode semiconductor lasers with optical feedback,” *J. Opt. B: Quantum Semiclassical Opt.*, vol. 4, no. 6, p. 415, 2002.

[59] I. V. Koryukin and P. Mandel, “Dynamics of semiconductor lasers with optical feedback: Comparison of multimode models in the low-frequency fluctuation regime,” *Phys. Rev. A*, vol. 70, no. 5, pp. 218–221, 2004.

[60] F.-Y. Lin and J.-M. Liu, “Diverse waveform generation using semiconductor lasers for radar and microwave applications,” *IEEE J. Quantum Electron.*, vol. 40, no. 6, pp. 682–689, Jun. 2004.

[61] D. Rontani, A. Locquet, M. Sciamanna, D. S. Citrin, and S. Ortin, “Time-delay identification in a chaotic semiconductor laser with optical feedback: A dynamical point of view,” *IEEE J. Quantum Electron.*, vol. 45, no. 7, pp. 879–1891, Jul. 2009.

[62] H. Huang *et al.*, “Multimode optical feedback dynamics of InAs/GaAs quantum-dot lasers emitting on different lasing states,” *AIP Adv.*, vol. 6, no. 12, 2016, Art. no. 125114.

[63] A. Quirce, Á. Valle, H. Thienpont, and K. Panajotov, “Enhancement of chaos bandwidth in VCSELs induced by simultaneous orthogonal optical injection and optical feedback,” *IEEE J. Quantum Electron.*, vol. 52, no. 10, Oct. 2016, Art. no. 2400609.

[64] F. Grillot, N. Naderi, M. Pochet, C.-Y. Lin, and L. Lester, “Variation of the feedback sensitivity in a 1.55 $\mu$m InAs/InP quantum-dash Fabry–Perot semiconductor laser,” *Appl. Phys. Lett.*, vol. 93, no. 19, 2008, Art. no. 191108.

[65] A. Capua *et al.*, “Direct correlation between a highly damped modulation response and ultra low relative intensity noise in an InAs/GaAs quantum dot laser,” *Opt. Express*, vol. 15, no. 9, pp. 5388–5393, 2007.

[66] N. Schunk and K. Petermann, “Numerical analysis of the feedback regimes for a single-mode semiconductor laser with external feedback,” *IEEE J. Quantum Electron.*, vol. 24, no. 7, pp. 1242–1247, Jul. 1988.

[67] O. Qasaimeh *et al.*, “Bistability and self-pulsation in quantum-dot lasers with intracavity quantum-dot saturable absorbers,” *Appl. Phys. Lett.*, vol. 74, no. 12, pp. 1654–1656, 1999.

[68] H. D. Summers, D. R. Matthews, P. M. Smowton, P. Rees, and M. Hopkinson, “Laser dynamics in self-pulsating quantum dot systems,” *J. Appl. Phys.*, vol. 95, no. 3, pp. 1036–1041, 2004.

[69] E. A. Viktorov *et al.*, “Low-frequency fluctuations in two-state quantum dot lasers,” *Opt. Lett.*, vol. 31, no. 15, pp. 2302–2304, 2006.

[70] E. A. Viktorov *et al.*, “Dynamics of a two-state quantum dot laser with saturable absorber,” *Appl. Phys. Lett.*, vol. 90, no. 12, 2007, Art. no. 121113.

[71] S. Mokkapati, H. H. Tan, C. Jagadish, and M. Buda, “Self-sustained output power pulsations in InGaAs quantum dot ridge-waveguide lasers,” *Appl. Phys. Lett.*, vol. 92, no. 2, 2008, Art. no. 021104.

[72] S.-C. Chan, S.-K. Hwang, and J.-M. Liu, “Period-one oscillation for photonic microwave transmission using an optically injected semiconductor laser,” *Opt. Express*, vol. 15, no. 22, pp. 14921–14935, 2007.

[73] A. Owen, P. Rees, I. Pierce, D. Matthews, and H. Summers, “Theory of Q-switching in a quantum-dot laser diode,” *Proc. Inst. Elect. Eng.—Optoelectron.*, vol. 150, no. 2, pp. 152–158, 2003.

[74] J.-P. Zhuang and S.-C. Chan, “Tunable photonic microwave generation using optically injected semiconductor laser dynamics with optical feedback stabilization,” *Opt. Lett.*, vol. 38, no. 3, pp. 344–346, 2013.

[75] Y.-H. Hung and S.-K. Hwang, “Photonic microwave amplification for radio-over-fiber links using period-one nonlinear dynamics of semiconductor lasers.” *Opt. Lett.*, vol. 38, no. 17, pp. 3355–3358, 2013.

[76] T. B. Simpson, J. M. Liu, M. Almulla, N. G. Usechak, and V. Kovanis, “Limit-cycle dynamics with reduced sensitivity to perturbations,” *Phys. Rev. Lett.*, vol. 112, no. 2, 2014, Art. no. 023901.

[77] C. Wang *et al.*, “Optically injected InAs/GaAs quantum dot laser for tunable photonic microwave generation,” *Opt. Lett.*, vol. 41, no. 6, pp. 1153–1156, 2016.

**Yue-Guang Zhou** was born in Lianyuan, China, in 1995. He received the bachelor’s degree in electronic science and technology from the Harbin Institute of Technology, Harbin, China, in 2017. He is currently working toward the master’s degree with the School of Information Science and Technology, ShanghaiTech University, Shanghai, China. His current research interests include modeling and characterization of quantum dot lasers.

**Jianan Duan** was born in Yinchuan, China, in 1992. He received the bachelor’s degree in optronics engineering from the Huazhong University of Science and Technology, Wuhan, China, in 2014, the Engineer Diploma in optronics from the University of Paris-Sud, Orasy, France, in 2016, and the master’s degree in electronics from the University of Paris-Saclay, Saclay, France, in 2016. He is currently working toward the Ph.D. degree with the Department of Communication and Electronics, Télécom Paris-Tech, Paris, France. His current research interests are focused on the study of the dynamics of quantum dot lasers.

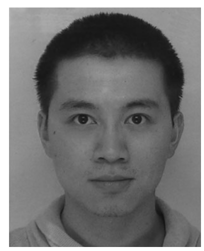

**Heming Huang** was born in Bengbu, China, in 1989. He received the engineer degree in material science and engineering and the M.Sc. degree in photonics from the Institut National des Sciences Appliquees, Rennes, France, in 2013, and the Ph.D. degree from Telecom ParisTech, Paris, France, in 2017. His doctoral research activities were conducted, within Com-Elec Department, on the nonlinear dynamics of the quantum dot lasers for fiber-optic communication. He then rejoined Telecom ParisTech to pursue his research. His main research interests include optical chaos for fiber-based secured communication links, optical feedback dynamics and phase noise properties for silicon photonics applications, and fundamental studies on quantum dot lasers operating on excited-state transition.

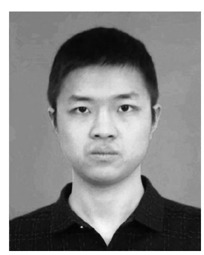

**Xu-Yi Zhao** was born in Ezhou, China in 1994. He received the M.S. degree in condensed physics from Shanghai University, Shanghai, China, in 2018. During his master period, he was a Joint Master Student with the Shanghai Institute of Microsystem and Information Technology. Since 2018, he has been a Research Intern with the Shanghai Institute of Microsystem and Information Technology. His main research interests are design and molecular beam epitaxy growth of semiconductor-based devices for applications in optical communication.

**Chun-Fang Cao** was born in Suzhou, China, in 1981. She received the bachelor’s degree in optoelectronic science and technology from the Changchun University of Technology, Jilin, China, in 2004, and the M.S. degree in optics from Zhejiang University, Hangzhou, China, in 2006. Since 2006, she has been an Assistant Professor with the Shanghai Institute of Microsystem and Information Technology, Chinese Academy of Sciences, Shanghai, China. Her current research interests are focused on characterization and device processing technology of semiconductor lasers.

**Qian Gong** received the B.S. degree in applied physics from Beijing Normal University, Beijing, China, in 1993, and the Ph.D. degree from the Institute of Semiconductors, Chinese Academy of Sciences, Beijing, in 1998. From 1999 to 2001, he was with the Paul Drude Institute for Solid State Electronics, Berlin, Germany, where his research involved investigation of molecular beam epitaxy of low-dimensional semiconductor structures. From 2001 to 2004, he was with the COBRA Inter-University Research Institute, Eindhoven University of Technology, Eindhoven, The Netherlands, working on molecular beam epitaxy of InAs quantum dots on GaAs and InP substrates, respectively. In 2004, he joined the Shanghai Institute of Microsystem and Information Technology, Chinese Academy of Sciences, Shanghai, China. His current research interests include molecular beam epitaxy of semiconductor materials, single-mode lasers, optical integration on Si, and external cavity tunable semiconductor lasers.

**Frédéric Grillot** was born in Versailles, France, on August 22, 1974. He received the M.Sc. degree in physics from the University of Dijon, Dijon, France, in 1999, the Ph.D. degree in electrical engineering from the University of Besançon, Besançon, France, in 2003, and the Research Habilitation in physics from the University of Paris VII, Paris, France, in 2012. His doctoral research activities were conducted within the Optical Component Research Department, Nokia Bell Labs (formerly Alcatel-Lucent) working on the effects of the optical feedback dynamics in semiconductor lasers, and the impact of this phenomenon on communication systems. From 2003 to 2004, he was with the Center for Nanoscience and Nanotechnology, University of Paris-Saclay, where he focused on integrated optics modeling and silicon-based passive devices for optical interconnects. Between 2004 and 2012, he was an Assistant Professor with the Institut National des Sciences Appliquées, Rennes, France. From 2008 to 2009, he was a Visiting Research Professor with the University of New Mexico, Albuquerque, NM, USA, leading research in optoelectronics with the Center for High Technology Materials. In October 2012, he joined Télécom ParisTech, Paris, one of the top French public institutions of higher education and research of engineering in France, as an Associate Professor and became a Full Professor in January 2017. Since August 2015, he has also been a Research Professor with the University of New Mexico. During April–December 2017, he joined the Department of Electrical Engineering, University of California, Los Angeles, CA, USA, as a Visiting Professor teaching dynamics of lasers and applied quantum mechanics. He has authored or coauthored 90 journal articles, one book, three book chapters, and more than 200 contributions in international conferences and workshops. His current research interests include, but are not limited to, advanced quantum-confined devices using new materials such as quantum dots and dashes, light emitters based on intersubband transitions, nonlinear dynamics, and optical chaos in semiconductor lasers systems, as well as microwave and silicon photonics applications. He is currently an Associate Editor for *Optics Express* and a Senior Consultant & Advisor Technology Partnerships for Baehl Innovation. He is a Fellow of the SPIE and a Senior Member of the IEEE Photonics Society.

**Cheng Wang** was born in Tengzhou, China in 1987. He received the M.S. degree in physical electronics from the Harbin Institute of Technology, Harbin, China, in 2011, and the Ph.D. degree in optoelectronics from the Institut National des Sciences Appliquées, Rennes, France, in 2015. During his Ph.D. period, he has researched at Télécom ParisTech, Paris, France, Technische Universität Berlin, Germany, and the Politecnico di Torino, Italy. He then joined the Department of Electronic Engineering, City University of Hong Kong, Hong Kong, as a Senior Research Assistant. Since 2016, he has been a Tenure-Track Assistant Professor with ShanghaiTech University, Shanghai, China. His main research interests are modeling and characterization of quantum-structured semiconductor lasers including quantum dot lasers, quantum cascade lasers, and interband cascade lasers, for applications in optical communication and in gas spectroscopy.